The Journal of Neuroscience, March 1991, 11(3): 869–880

A Mouse Brain Homolog of the *Drosophila Shab* K+ Channel with Conserved Delayed-Rectifier Properties

Michael D. Pak,[1] Manuel Covarrubias,[1] Ann Ratcliffe,[1] and Lawrence Salkoff[1,2]

[1]Department of Anatomy and Neurobiology and [2]Department of Genetics, Washington University School of Medicine, St. Louis, Missouri 63110

We have cloned and expressed a mouse brain K+ channel that is the homolog of the *Drosophila Shab* K+ channel. Mouse and *Drosophila Shab* K+ channels (*mShab* and *fShab*, respectively) represent an instance of K+ channels in distantly related species that are both functionally and structurally conserved; most kinetic, voltage-sensitive, and pharmacological properties are similar for the 2 channels. The greatest functional difference between the currents is recovery from inactivation, which is several times slower for *mShab* than for *fShab* currents. In addition to conserved structure, the *mShab* polypeptide has an unusually long nonconserved region at the carboxyl end of the protein. Truncation of 293 residues from the carboxyl end produced no noticeable change in voltage-sensitive, kinetic, or pharmacological properties. Thus, the measured functional properties of *mShab* are determined by the remaining 564 residues, most of which are conserved. The *mShab* and *fShab* channels are naturally occurring structural variants having substitutions in conserved portions that appear relatively neutral with respect to all measured properties except for, possibly, the rate of recovery from inactivation. The *mShab* current closely resembles a native delayed-rectifier-type potassium current, I_K, in hippocampal neurons.

Potassium channel diversity is generated by an extended gene family encoding homologous channel proteins. An extended gene family consisting of 4 distinct members was originally isolated from *Drosophila* (Tempel et al., 1987; Kamb et al., 1988; Pongs et al., 1988; Butler et al., 1989; Wei et al., 1990). Each *Drosophila* gene, *Shaker, Shab, Shaw,* and *Shal,* is conserved in mammals (Baumann et al., 1988; Tempel et al., 1988; Frech et al., 1989; Yokoyama et al., 1989; Wei et al., 1990), where some are present as multigene subfamilies.

cDNAs from at least 6 mammalian *Shaker* subfamily genes have been isolated and expressed in the *Xenopus* expression system (Baumann et al., 1988; Stuhmer et al., 1988, 1989; Tempel et al., 1988; Christie et al., 1989, 1990; McKinnon, 1989; Yokoyama et al., 1989; Chandy et al., 1990; Grupe et al., 1990; Koren et al., 1990; Swanson et al., 1990). However, none of the currents expressed by the mammalian *Shaker* homologs closely resembles the *Shaker* current from *Drosophila*; most mammalian currents of *Shaker* homologs undergo slow inactivation and have been categorized as "delayed-rectifier" channels. The *Drosophila Shaker* current, in contrast, is a transient, A-type K+ current (Connor and Stevens, 1971; Salkoff, 1983; Solc et al., 1987; Iverson et al., 1988; Timpe et al., 1988a,b). Although one of the mammalian *Shaker* currents, *RCK4,* does show rapid inactivation, it differs significantly from the *Drosophila* A-current in its voltage-sensitive properties (Stuhmer et al., 1989).

We show, however, that the mouse and *Drosophila* homologs of *Shab* K+ channels (*mShab* and *fShab*) represent an instance of homologs in distantly related species that are functionally as well as structurally conserved. This is true with regard to their voltage-sensitive properties and most kinetic and pharmacological properties. The properties of the *mShab* current also closely match those of one type of delayed rectifier current, I_K, observed in the rat hippocampus. Unlike the mammalian *Shaker* type of delayed-rectifier currents, which activate very rapidly, *mShab* and *fShab* currents activate more slowly. *mShab* and *fShab* currents also differ from the mammalian *Shaker* currents in that they are insensitive to 4-aminopyridine (4-AP). *mShab* and *fShab* currents are distinct from a previously expressed homolog of *Drosophila Shab* isolated from the rat brain, *drk1* (Frech et al., 1989).

Materials and Methods

Screening of the mouse brain cDNA library. A mouse brain cDNA library kindly provided by J. Merlie was screened using a degenerate synthetic oligonucleotide probe ($CG^A/_GTC^A/_GAA^A/_GAA^A/_GTA^T/_CTC^G/_ATT$) based on a highly conserved region (*mShab1* residues 81–87; Fig. 1). Oligonucleotides were end labeled with ^{32}P using T-4 nucleotide kinase (Maniatis et al., 1982). Hybridization conditions were 5 × SSPE (1.1 M NaCl, 60 mM NaH_2PO_4, 6 mM Na_2EDTA, pH 7.7), 5 × Denhardt's, and 0.5% SDS at 42°C for 12 hr; filters were washed in 1 × SSC (Maniatis et al., 1982) with 0.1% SDS at 25°C. The first *mShab* cDNA isolated was incomplete and was used as a probe, under conditions of high stringency, to isolate the full-length clone *mShab1.* The high-stringency conditions were 5 × SSPE, 5 × Denhardt's, and 0.5% SDS at 65°C for 12 hr followed by a wash in 0.1 × SSC with 0.1% SDS at 55°C.

Nucleotide sequence determination and analysis. The *mShab1* cDNA was subcloned into both M13mp18 and pBluescriptII SK+ vectors (Stratagene). Both single-stranded and double-stranded DNAs were used as templates, and bidirectional sequencing was performed using the dideoxy technique (Sanger et al., 1977). Sequences were analyzed using MICROGENIE software (Beckman). The truncated $mShab1^{\Delta 565}$ was sequenced and analyzed in a similar manner.

Vector construction and cRNA synthesis. mShab1, $mShab1^{\Delta 565}$, and *fShab* cDNAs were subcloned into plasmid vectors (pBluescript II SK+,

Received May 14, 1990; revised Aug. 30, 1990; accepted Oct. 11, 1990.

We thank A. Butler for technical help and A. Wei, K. Baker, and E. McCleskey for many helpful suggestions. We also thank J. Merlie for the generous gift of a cDNA library. This research is supported by NIH 1 RO1NS24785-01 and by grants from the Muscular Dystrophy Association of America and from Monsanto-Searle. M.D.P. is supported by Training Grant NS07071-11.

Correspondence should be addressed to Lawrence Salkoff, Department of Anatomy and Neurobiology, Box 8108-WUMS, 660 South Euclid Avenue, St. Louis, MO 63110.

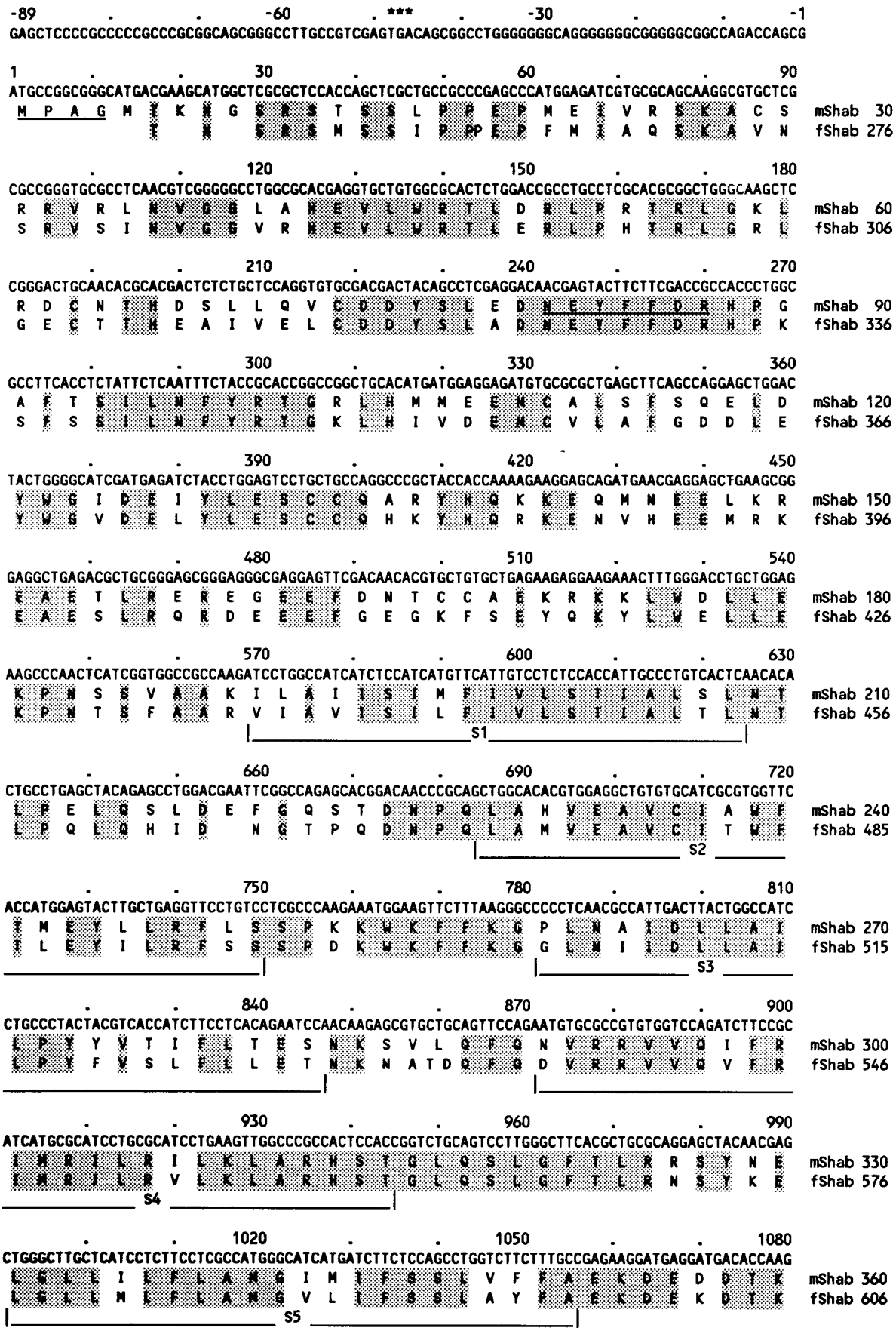

Figure 1. Sequence comparisons of *Shab* proteins: nucleotide and deduced amino acid sequence of *mShab1* and its comparison to *fShab* and *drk1*. Identical amino acid residues common to both *mShab1* and *fShab* are *shaded*. Amino acid residues that differ between *mShab1* and *drk1* are shown below the corresponding *mShab1* residues; the *drk1* residues are shown in *parentheses*. The first stop codon upstream and in frame with the designated translation initiator methionine codon is marked with *asterisks* (***). The *mShab1* amino acid residues *1–4* (*underlined*) are not present in the deduced *drk1* protein sequence. The *underlined* amino acid residues *81–87* are conserved in most K^+ channels. The SphI restriction

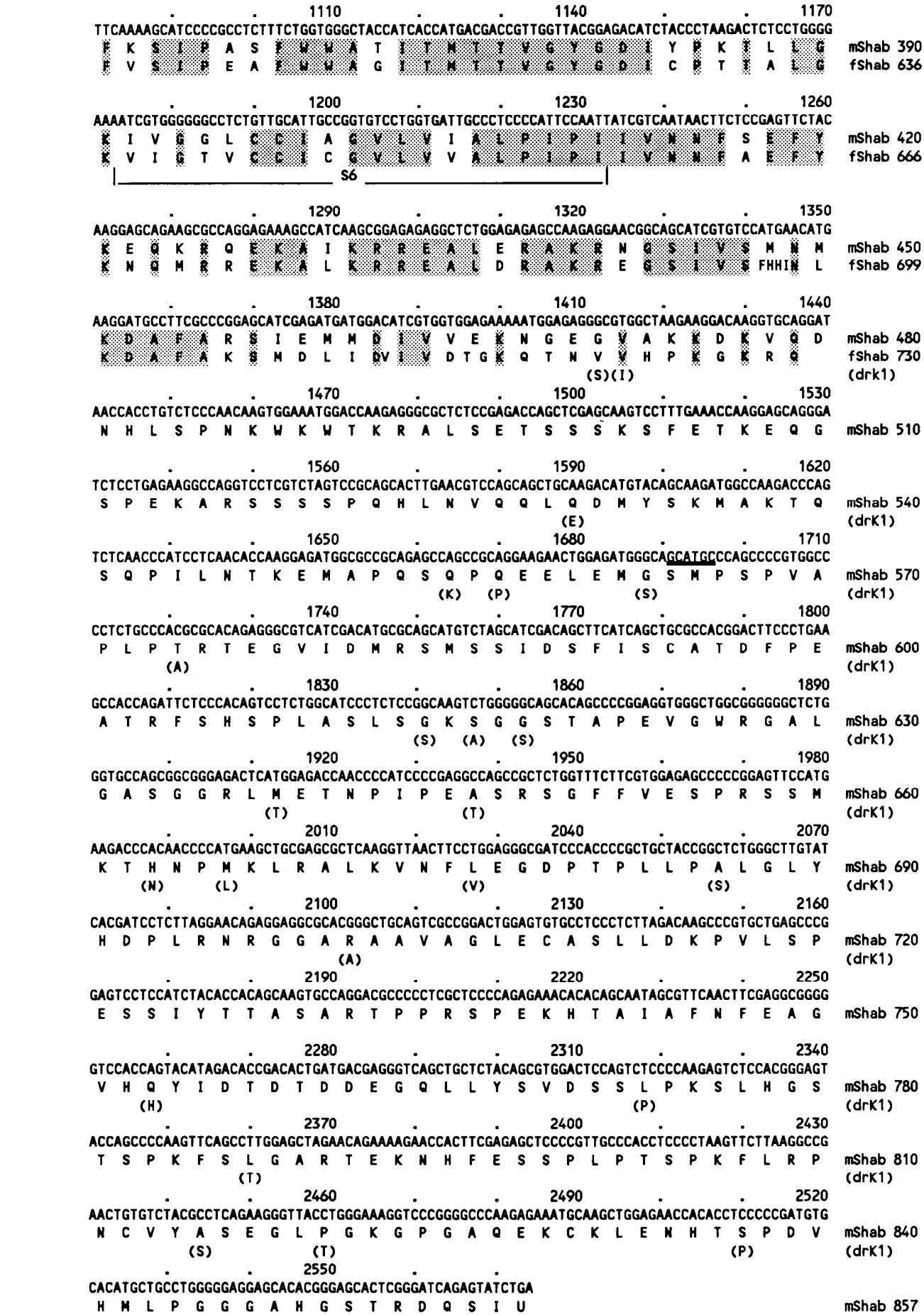

site (1691; *mShab1*$^{\Delta 565}$ truncation site) is *double underlined.* This figure contains the corrected version of the *Shab11* amino acid residues 626–627 and 681–702 (Butler et al., 1990).

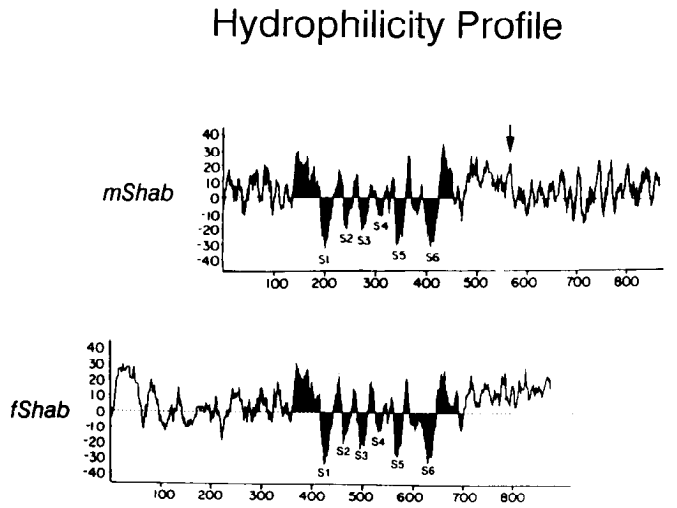

Figure 2. Hydrophilicity profile of *mShab1* and *fShab*. Profiles were computed according to Kyte and Doolittle (1982) with a window size of 9 amino acids. Negative (*downward*) index values indicate hydrophobic groups, while positive values indicate hydrophilic groups. The truncation site to create $mShab1^{\Delta 565}$ is indicated by an *arrow*.

Stratagene), which served as template for *in vitro* transcription reactions. The *mShab1* construct included the sequence shown in Figure 1 and an additional 800 base pairs (bp) of a 3′ untranslated region. The *fShab* cDNA is the *Shab11* cDNA (Butler et al., 1990). Expression was enhanced by the replacement of the original translational start site with the consensus translation initiation sequence CCACCATGG (Kozak, 1986). The $mShab1^{\Delta 565}$ cDNA was made from the *mShab1* cDNA by cleaving at the SphI site (Fig. 1, 1691) and removing the downstream sequence. A 200-bp fragment containing the 3′ untranslated sequence and the translation stop signal was added at the SphI site. The polymerase chain reaction technique (Perkin Elmer; Saiki et al., 1985) was used to synthesize this fragment.

Capped cRNA for both *mShab1* and *fShab* was synthesized *in vitro* as previously reported (Wei et al., 1990). The transcription reaction contained 3 μg of linearized template DNA, 1 mM nucleotide triphosphates, 1 mM 7mG(5′)ppp(5′)G (cap analog; New England Biolab), and 20 U T3 RNA polymerase, in supplied (Stratagene) transcription buffer and was incubated at 37°C for 1 hr.

Expression of cRNAs in Xenopus *oocytes.* Oocytes were injected with ~50 nl (approximately 100 ng) cRNA in water and incubated in ND96 (as below, plus 1.8 mM $CaCl_2$), supplemented with 2.5 mM sodium pyruvate, penicillin (100 U/ml), and streptomycin (100 μg/ml), at 19°C for 2–4 d. Prior to injection with cRNA, *Xenopus laevis* oocytes (stage 4–6) were incubated for 2 hr in collagenase (1 mg/ml; type IA, Sigma) in ND96 without Ca^{2+} (96 mM NaCl, 2 mM KCl, 1 mM $MgCl_2$, 5 mM HEPES, pH 7.5). Macroscopic currents were recorded in ND96 using a conventional 2-microelectrode voltage clamp. One mM 4,4′-diisothiocyanatostilbene-2,2′-disulfonic acid (DIDS; Calbiochem) was added to block the endogenous Ca^{2+}-dependent Cl^- current. Current records were filtered at 0.5 or 1 kHz with an 8-pole Bessel filter, acquired digitally with CCURRENT, and analyzed using CQUANT (software written by Keith Baker). Curve fitting was done using nonlinear least-square fitting routines (CQUANT and NFIT, Island Products). Recordings were performed at room temperature (21–24°C) or at 15°C using a Peltier device (Cambion).

Results

Isolation and sequencing of Shab *clones*

A full-length *mShab* clone (*mShab1*) was isolated by taking advantage of a sequence of 7 amino acids upstream of the S1 transmembrane region found to be conserved in most potassium channels (Fig. 1, *mShab* 81–87). A degenerate oligonucleotide probe based on these 7 amino acids was used to screen a mouse brain cDNA library. A 1.7-kilobase (kb) 5′-biased cDNA clone was isolated and subcloned into an M13mp18 vector. Single-stranded sequencing using the same degenerate oligonucleotide as a primer revealed homology with the *Drosophila Shab* gene (Butler et al., 1989). Further sequencing revealed that this clone was truncated at the 3′ end between the S1 and S2 transmembrane region by a natural EcoRI site (Fig. 1, 655). A larger cDNA of approximately 3.5 kb containing the complete translated region was isolated using the 5′-biased cDNA as a probe to screen the same library. The cDNA inserts were subcloned into M13mp18 and Bluescript vectors for sequencing. The isolation of the *Drosophila Shab11* (*fShab*) cDNA was reported previously (Butler et al., 1989).

Sequence analysis and primary structure of mShab1

The full-length *mShab* cDNA, *mShab1*, has an open reading frame of 2571 nucleotides, which encodes a protein of 857 amino acid residues of MW 96,000 (Fig. 1). The putative translation initiation codon is the first ATG triplet upstream in the longest open reading frame. Upstream from this ATG translation start site, the reading frame is closed by a TGA stop signal (Fig. 1). The 5′ untranslated region extends approximately 1.0 kb upstream of the assigned initiation codon and may not represent the complete 5′ end of the transcript. The sequence surrounding the assigned initiation methionine (CCAGCGATGC) agrees at 6 of 10 sites with the consensus sequence for eukaryotic initiation ($GCC^A/_GCCATGG$; Kozak, 1986, 1987, 1989); the important purine residue (G) is present at −3. The open reading frame is terminated by a TGA codon at position 2572, followed by approximately 800 bp of 3′ untranslated region. A polyadenylation signal, AATAAA (Proudfoot and Brownlee, 1976) is present, as well as a polyA tail of 22 nucleotides.

The *mShab1* and *fShab* conceptual proteins have very similar hydrophilicity profiles in the central core region containing the 6 putative hydrophobic transmembrane regions S1–S6 (Fig. 2). The similarity of profiles for the intramembrane regions sharply contrasts with the lack of similarity seen in the terminal regions. It can be seen from Figure 2 that the relative position of the conserved core within the protein as a whole differs considerably between *mShab1* and *fShab*; for *mShab1*, the conserved core is much closer to the N-terminal and resembles most other cloned K^+ channels in this regard (Schwarz et al., 1988; Butler et al., 1989; Stuhmer et al., 1989).

The degree of identity between *mShab1* and *fShab* is approximately 70% over the conserved region (Fig. 1). This is in contrast to an average of approximately 38% when comparing the percent identity of either *Shab* protein with a *Shaker* protein from either fly or mouse (Wei et al., 1990). The total conservation between *mShab1* and *fShab* over the area compared in Figure 1 is approximately 83%.

Differences are present between *mShab1* and *fShab* outside of the central core region. The *mShab1* peptide has an extended C-terminal portion, whereas the *fShab* peptide has a longer N-terminal portion. The homology between *mShab1* and *fShab* begins close to the initiator methionine of *mShab1* (Fig. 1; *mShab* 6). Because of the large nonconserved N-terminal extension of *fShab* (Butler et al., 1989), the conserved portion of the protein in *fShab* begins 253 residues downstream from the initiator methionine in the fly protein. Notably, the *mShab1* initiation site is at the border of conservation shared by all 4 K^+ channel subfamilies, *Shab, Shaker, Shaw,* and *Shal.*

Asparagine-linked glycosylation consensus sequences ($NX^T/_S$; Kornfeld and Kornfeld, 1985) are found in a similar position

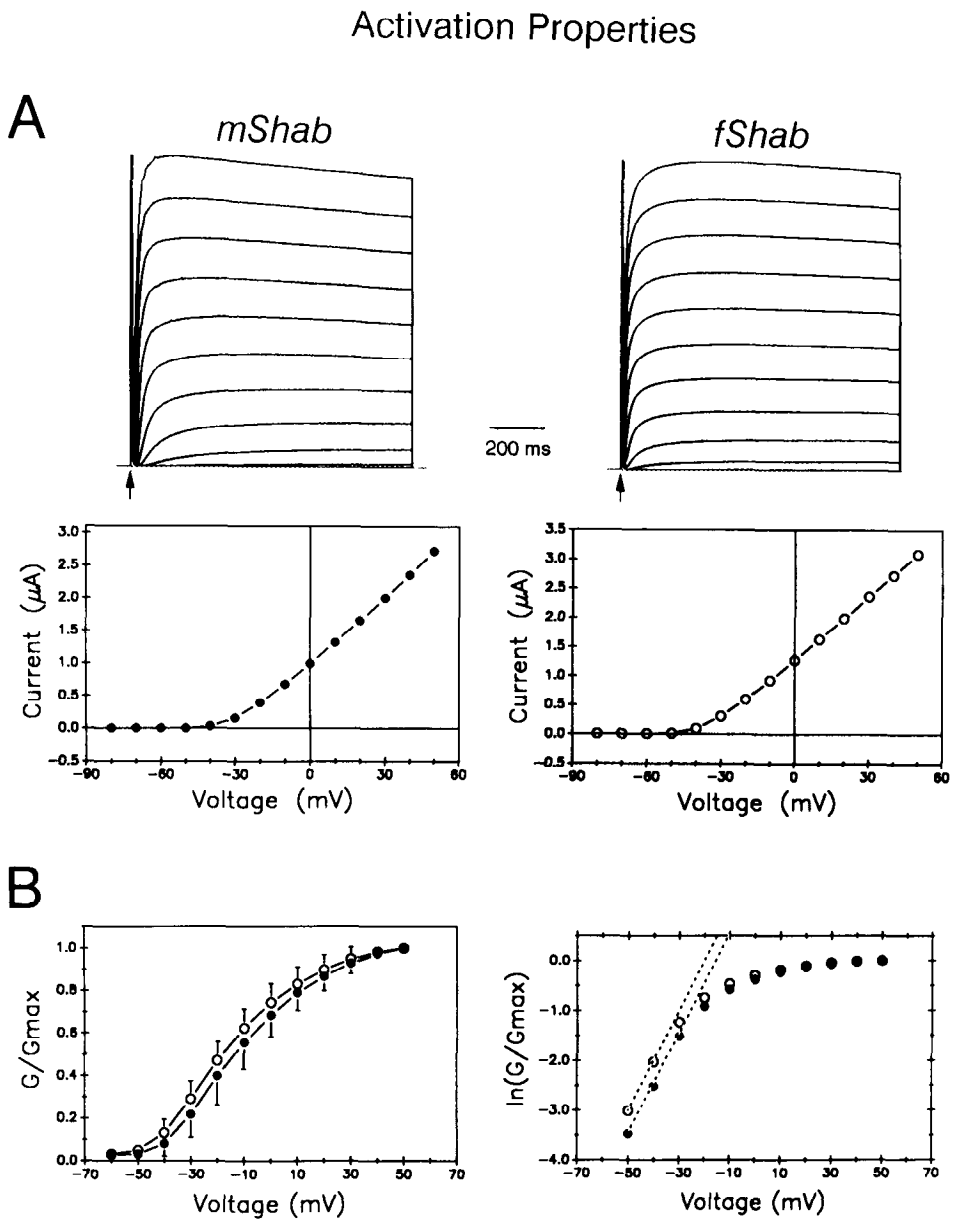

Figure 3. Activation properties of *mShab* and *fShab* currents. *A,* Comparison of current-voltage relationships of *mShab1* (*left*) and *fShab* (*right*) expressed in *Xenopus* oocytes. Voltage-clamp currents (*upper traces*) are shown in response to 1 sec depolarizing pulses from a holding potential of −90 mV. The membrane was depolarized in increments of 10 mV until a membrane potential of +50 mV was reached. *Arrows* indicate onset of the voltage jump. The currents were linear leak subtracted, but the capacitative current was not subtracted. The interval between trials was 10 sec. Because the *mShab1* current recovers from inactivation more slowly than the *fShab* current (see Results), the membrane was hyperpolarized to −120 mV for 5 sec during the initial half of the interval between trials in *mShab1* experiments to speed up recovery from inactivation. Because the recovery process is steeply voltage dependent (see Results), virtually all *mShab1* channels are available for activation at the end of the 5-sec prepulse at −120 mV. The results for *mShab1* were the same when the membrane was at −90 mV during the interval between trials; however, the interval between trials had to be lengthened to allow all the channels to recover from inactivation (15–20 sec). Peak current–voltage relationships are plotted *below* the current traces. Notice the sharp voltage responsiveness of both channels at approximately −50 mV. *B,* Peak conductance–voltage relationships for *mShab1* (*solid circles*) and *fShab* (*open circles*). *Left,* the peak membrane conductance (G) was calculated for a given command voltage (V_c) and peak current response (I_{peak}) from the expression $G = I_{peak}/(V_c - V_r)$, where V_r is the 0 current membrane potential for a given channel. V_r was measured from tail current analysis and was determined to be between −90 and −80 mV for all the studied cells (see Fig. 7). Instantaneous current–voltage relationships were approximately linear in the studied voltage range, as determined by similar experiments. G was normalized to the peak membrane conductance at +50 mV (G_{max}). Each *symbol* is the mean ±SD of 6 and 10 oocytes injected with *mShab1* or *fShab* cRNA, respectively. The membrane reached half-maximal conductance at similar voltages for both *mShab1* and *fShab* (−14 and −19 mV, respectively). *Right,* mean values (G/G_{max}) were plotted as $\ln(G/G_{max})$ versus command voltage (Hodgkin and Huxley, 1952a). The slopes (*dotted lines*) between −50 and −40 mV were calculated to estimate the limiting equivalent voltage sensitivity of the channels; the activation of both currents appears equally voltage sensitive (10 mV/*e*-fold).

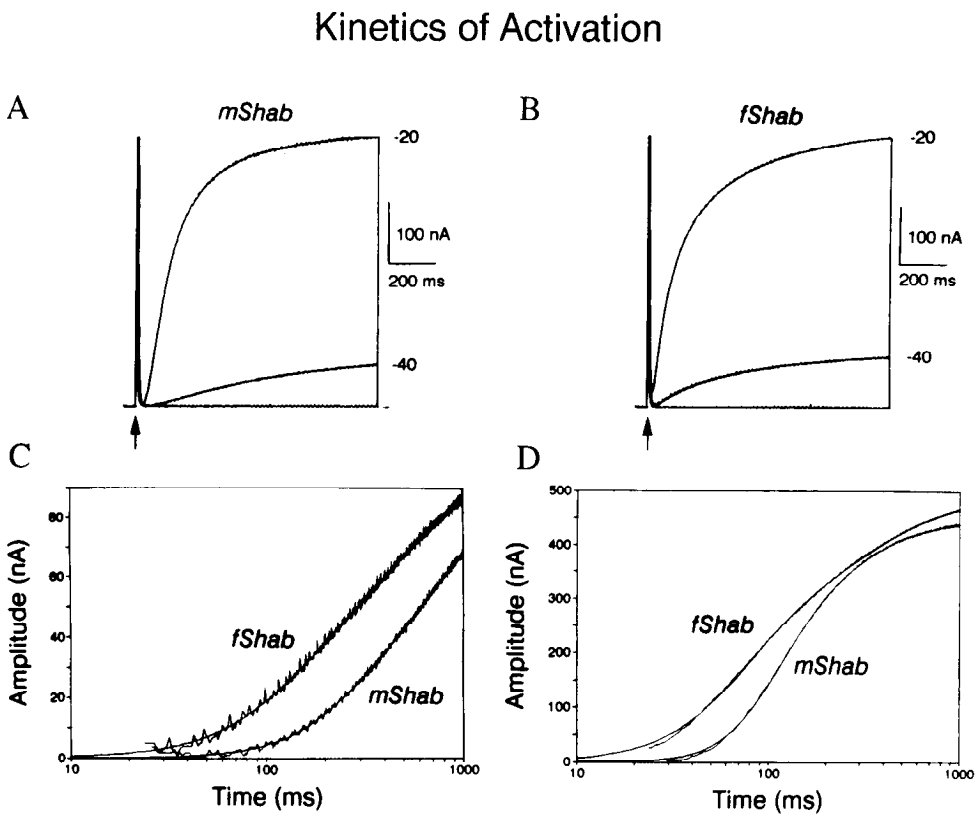

Figure 4. Kinetics of current rise time at low membrane voltages. *A* and *B*, Current responses to 1-sec depolarizing voltage step pulses from a holding potential of −90 mV. *A*, *mShab1*; *B*, *fShab*. *Arrows* indicate pulse onset. Currents were corrected assuming a linear leak; capacitative current was not subtracted. Experiments were carried out at 15°C. Notice the longer activation delay of *mShab1* currents. *C* and *D*, Current traces from *A* and *B* plotted on a log time scale at −40 mV (*C*) and at −20 mV (*D*). *Lines* through the data (excluding the capacitative current) show best fits to a 2-component exponential function,

$$I = A_1[1 - \exp(-t/T_1)]^{n1} + A_2[1 - \exp(-t/T_2)]^{n2},$$

where I is the total current response, A_1 and A_2 are the amplitudes of the components, and T_1 and T_2 are time constants. *mShab1* best-fit parameters at −40 mV are A_1 = 10.8 nA, T_1 = 107 msec, $n1$ = 5.4, A_2 = 75.2 nA, T_2 = 519.2 msec, and $n2$ = 1.7. *fShab* best fit parameters at −40 mV are A_1 = 22.2 nA, T_1 = 77.1 msec, $n1$ = 2.6, A_2 = 71.7 nA, T_2 = 405.6 msec, and $n2$ = 1.4. *mShab1* best fit parameters at −20 mV are A_1 = 279.2 nA, T_1 = 52.8 msec, $n1$ = 4.9, A_2 = 160.4 nA, T_2 = 193.4 msec, and $n2$ = 2.5. *fShab* best fit parameters at −20 mV are A_1 = 226.2 nA, T_1 = 45.5 msec, $n1$ = 2.5, A_2 = 246 nA, T_2 = 274.8 msec, and $n2$ = 1.3. The higher powers of the exponential terms describing *mShab1* activation are consistent with a more prolonged delay of current activation (Hodgkin and Huxley, 1952b).

between S3 and S4 in both *mShab1* and *fShab* (Fig. 1, *mShab* 283, *fShab* 530). One consensus site conserved in most K^+ channel families is found in the segment linking S1 and S2 (Butler et al., 1989); this site, present in *fShab*, is not found in *mShab1* (Fig. 1, *fShab* 465). It is presently unknown whether native *Shab* channels are glycosylated.

Potential cAMP-dependent phosphorylation sites ($^{Arg}/_{Lys}$-$^{Arg}/_{Lys}$-*X*-$^{Ser}/_{Thr}$ or $^{Arg}/_{Lys}$-$^{Arg}/_{Lys}$-*X*-*X*-$^{Ser}/_{Thr}$; Krebs and Beavo, 1979) are present in both *mShab1* and *fShab* on the carboxyl side of the S6 region. One of these sites is shared by both *mShab1* and *fShab* (Fig. 1; *mShab* 444, *fShab* 690), whereas another is at similar but not identical sites (*mShab* 496, Fig. 1; *Shab11* 731, Butler et al., 1990). The *fShab* has a third site (*Shab11* 796, Butler et al., 1990), whereas the *mShab1* has only 2 potential phosphorylation sites. One or more of these sites are conserved in all K^+ channels identified to date, which is proposed to be located on the cytoplasmic side in most models (Guy and Conti, 1990).

Functional expression: mShab1 *and* fShab *currents have similar current–voltage relations*

To compare the functional properties of *mShab1* and *fShab* currents, *Xenopus* oocytes were injected with either *mShab1* or *fShab* cRNA, incubated for approximately 48 hr, and then subjected to voltage-clamp analysis using the 2-microelectrode technique. Figure 3*A* shows *mShab1* and *fShab* currents evoked in response to a family of command pulses from −80 to +50 mV in 10-mV increments from a holding potential of −90 mV. A comparison of the current–voltage relation of *mShab1* and *fShab* currents is also shown. For both *mShab1* and *fShab* currents, net (leak subtracted) outward currents were detectable at command voltages more positive than −50 mV, which indicated a similar activation "threshold" for both currents. The current–voltage relation became linear for both *mShab1* and *fShab* currents between −20 and +40 mV.

To obtain additional information about the activation parameters of the currents, the normalized conductance–voltage relations were plotted for an average of 6 (*mShab1*) and 10 (*fShab*) injected oocytes (Fig. 3*B*, left graph). In both cases, the conductance rose sharply with depolarization and reached its half-maximal value between −15 to −20 mV. By plotting these data on a semilogarithmic graph (Fig. 3*B*, right graph), we found that *mShab1* and *fShab* channels had equal limiting equivalent voltage sensitivities (10 mV per *e*-fold change in conductance).

mShab1 *current activation is delayed relative to* fShab

Both *mShab1* and *fShab* currents display a relatively slow rate of current activation. However, a closer inspection of the rising phase of the currents at low voltages (Fig. 4) reveals that *mShab1* activates more slowly than *fShab*. To obtain a relative estimate of the difference, we measured the 10–90% current rise time at

Table 1. The functional properties of delayed-rectifier-type K^+ channels from *Drosophila* and rodents

Parameter	*mShab*	*fShab*	*mShab*$^{\Delta 565}$	*drk1*	I_K	*RCK1*
Activation	−50		−50	−15	−50	−40
"threshold" (mV)	(17)	−50	(6)			
$V_{0.5}$, activation (mV)[a]	−14	(24)	−12	—	—	−30
		−19	(2)			
Activation slope[a] (mV/*e*-fold)	10	10	—	—	—	7
Rise time[b]	584 ± 103	339 ± 83	—	200	400	16
(msec)	(6)	(9)				
τ, decay[c]	5.5 ± 2.8	9.2 ± 1.4	4.4	—	3	>3
(sec)	(5)	(9)	(2)			
τ, recovery[d]	4.2 ± 1.5	0.4 ± 0.2	3.5 ± 0.6	—	3	—
(sec)	(6)	(3)	(3)			
$V_{0.5}$, inactivation (mV)[e]	−45 ± 3.9	−45.5 ± 5.3	−45.3	—	−63	−47
	(6)	(5)	(1)			
Inactivation slope	6.7 ± 0.8	6.6 ± 1	6	—	—	4
(mV/*e*-fold)	(6)	(5)	(1)			
Selectivity[f]	55	53	—	48	>40	57
(mV/$\log_{10}$ mM)	(1)	(2)				
$K_{0.5}$, TEA[g]	5 ± 2	27 ± 5	10	10	10	0.6
(mM)	(3)	(3)	(2)			
$K_{0.5}$, 4-AP[g]	>100	>100	>100	0.5	>100	1
(mM)						

The number of experiments is shown in parentheses; error limits are ± SD. All of the values for *RCK1* were obtained from Stuhmer et al. (1989), their Table 1. The *drk1* values are from Frech et al. (1989); I_K values are from Segal and Barker (1984) unless otherwise noted.

[a] The voltage at which the conductance reached its half-maximal value. Activation slopes were estimated as limiting equivalent voltage sensitivity. The voltage at half-maximal conductance and the activation slope for *mShab* and *fShab* were obtained from Figure 3*B*. The activation values for *RCK1* were estimated from the best fit of the conductance–voltage relation to a Boltzmann isotherm (Stuhmer et al., 1989).

[b] A 10–90% rise time at temperatures that ranged between 20 and 24°C. Values for *RCK1* are measurements at 0 mV; for *drk1* at −10 mV; and for *mShab*, *fShab*, and I_K at −40 mV. *Drk1* rise time was estimated from Frech et al. (1989), their Figure 1*a*. I_K rise time was estimated from Segal and Barker (1984), their Figure 5*a*. The difference between *mShab* and *fShab* was statistically significant at $p < 0.001$ (2-tailed Student's *t* test).

[c] Time constant of current decay at temperatures that ranged between 20 and 24°C: *RCK1* at 0 mV, *mShab* and *fShab* at +20 mV, and I_K at −20 mV. The difference between *mShab* and *fShab* was statistically significant at $p < 0.005$ (2-tailed Student's *t* test).

[d] Time constant of recovery from inactivation at −90 mV. The temperature ranged between 21 and 24°C. The value for I_K (Storm, 1988) was estimated after correction for temperature and voltage dependence (assuming a Q_{10} of 3 and a voltage sensitivity of 28 mV/*e*-fold; see Results).

[e] The holding potential at which half of the channels are inactivated. This parameter and the inactivation slope were estimated from the best fit of the data to a Boltzmann isotherm (see Fig. 5 caption).

[f] Slope of the Nernst theoretical line in mV per 10-fold change in external K^+ concentration.

[g] The concentration of inhibitor necessary to block half of the current (see Fig. 8).

−40 mV, where slow current activation and the absence of inactivation allow accurate and reproducible measurements. A comparison of the 2 currents showed that *mShab1* required almost twice the time as *fShab* to activate (Table 1). This extra time required for *mShab1* current rise is due to slower kinetics of current activation. To describe the time course of current activation (Fig. 4), we fitted the data with an empirical exponential function (Hodgkin and Huxley, 1952b). For both *mShab1* and *fShab*, the data were best described by the sum of 2 powered exponential terms. However, to describe *mShab1* current activation, the exponential terms had to be raised to a higher power (see Fig. 4 caption). This reflected the substantially longer delay seen in *mShab1* activation (Fig. 4).

For both *mShab1* and *fShab* currents, the powers of the exponential terms needed to describe the delay of current activation were independent of voltage in the range of −40 to −20 mV (Fig. 4). This was true even though the overall rates of current activation increased at −20 mV relative to −40 mV. Similar results were obtained at 22°C; the powers of the exponential terms needed to describe the delay of current activation were the same as in 15°C experiments (even though the overall rates of current activation were faster).

Although the kinetics of current rise differ between *mShab1* and *fShab*, both currents activate at a rate substantially more slowly than the currents expressed by the mammalian homologs of *Shaker*, an example of which is *RCK1* (Table 1).

mShab1 *and* fShab *currents have similar prepulse inactivation properties, but the rate of recovery from inactivation differs*

Both *mShab1* and *fShab* currents display a clear decay phase during long depolarizing step pulses from a holding potential of −90 mV (Fig. 6). Although the rates of current decay are slow, they are well described by an exponential function with time constants measured in seconds (Table 1). *mShab1* and *fShab* currents showed a consistent difference in this property; when depolarized to +20 mV, the time constant of current decay for *mShab1* was about half that of *fShab*.

Although *mShab1* and *fShab* currents are different with regard to macroscopic inactivation rate, the voltage sensitivity of prepulse inactivation is similar. In Figure 5, the best fit to a Boltzmann isotherm indicated that both currents were half-inactivated at about −45 mV; the slope factor of both curves was approximately 7 mV per *e*-fold change in both cases (Table 1).

The rate of recovery from inactivation, however, greatly dif-

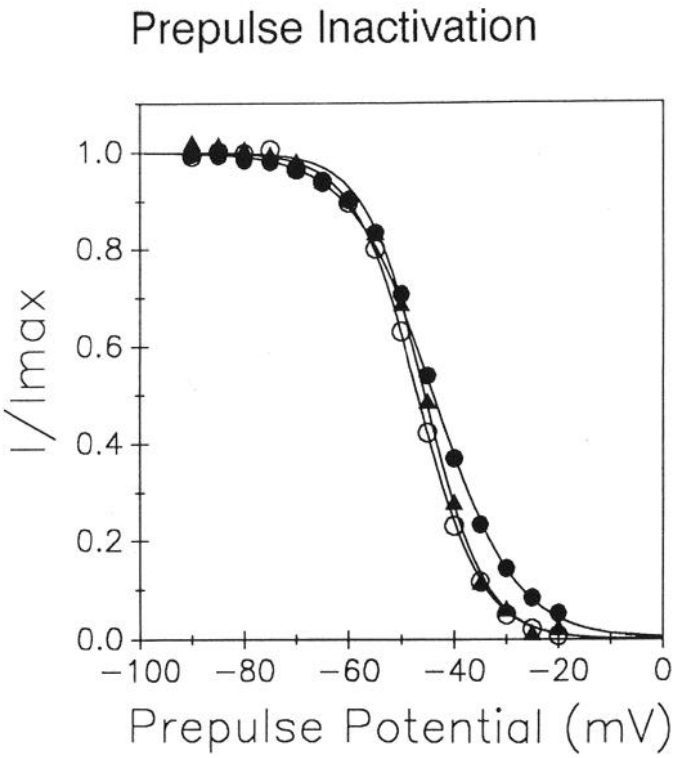

Figure 5. Similar prepulse inactivation properties for *mShab1* (*solid circles*), *mShab1*$^{\Delta 565}$ (*triangles*), and *fShab* (*open circles*). Currents were measured by a test pulse to +20 mV after a 10-sec prepulse. Prepulses were applied from −90 to −20 mV in increments of 5 mV. In the interpulse interval, the membrane was held at −90 mV for 10 sec for *fShab* or for 5 sec at −120 mV followed by 5 sec at −90 mV for *mShab1*. The additional interpulse hyperpolarization for *mShab1* was to insure the full recovery of these channels from inactivation (see Results). The *solid lines* are the best fit to a Boltzmann isotherm:

$$I = 1/(1 + \exp((V_h - V_{½})/a)) + b,$$

where $V_{½}$ is the prepulse potential (V_h) at which half of the activatable channels are inactivated, a is the slope factor, and b is the amount of current resistant to inactivation. For both *mShab1* and *fShab* channels, b was, on average, about 7% of the total current [the range was 5–11% (n = 6) and 4–13% (n = 5) for *mShab1* and *fShab*, respectively]. After subtracting b from I, the difference was normalized to the estimated maximal response (I_{max}). Best fit parameters: for *mShab1*, $V_{½}$ = −46.9 mV and a = 6.3 mV/e-fold; for *mShab1*$^{\Delta 565}$, $V_{½}$ = −45.3 mV and a = 6 mV/e-fold; for *fShab*, $V_{½}$ = −43.9 mV and a = 7.6 mV/e-fold.

fers for *mShab1* and *fShab* currents. This is shown in Figure 6*A*, where the response to a second identical voltage pulse is shown after an interval of 1 sec. For *fShab*, the response to the second pulse is virtually as large as the first. *mShab1*, in contrast, only recovered to about 25% of its original amplitude in response to the second pulse, which is less than the amplitude of the current at the end of the preceding pulse. This is most likely due to cumulative inactivation (Aldrich et al., 1979), which causes *mShab1* to recover more slowly than *fShab*. Indeed, at a holding potential of −90 mV, the recovery from inactivation was almost 10 times faster for *fShab* than for *mShab1* (Fig. 6*B*, Table 1).

Further investigation of recovery from inactivation for *mShab1* currents showed that the process was both steeply voltage and temperature dependent. Thus, at a more negative holding potential, −120 mV, the time constant decreased 3-fold to 1.4 ±

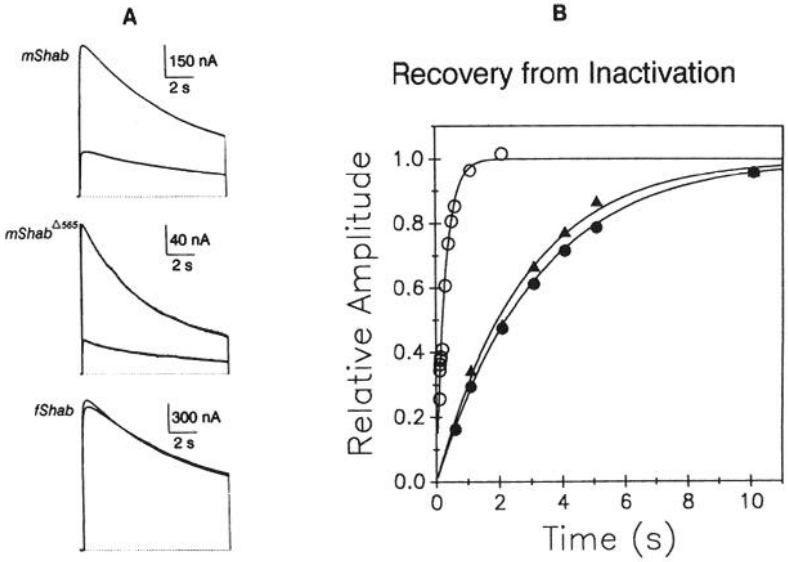

Figure 6. *A*, Kinetics of current decay and recovery from inactivation. Current traces are responses to twin 10-sec depolarizing pulses separated by an interpulse interval of 1 sec. Pulses were to +20 mV from a holding potential of −90 mV. The 3 currents, *mShab1*, *mShab1*$^{\Delta 565}$, and *fShab*, all show a slow decay. For *mShab1* and *mShab1*$^{\Delta 565}$, only 20–25% of the current amplitude recovered during the 1-sec interpulse interval; *fShab* fully recovered over the same period. *B*, Fraction of total current recovered as a function of interpulse interval duration (*mShab1*, *solid circles*; *mShab1*$^{\Delta 565}$, *triangles*; *fShab*, *open circles*). The holding potential was −90 mV. *Continuous lines* are best fits to a single exponential function. Estimated time constants are 3.2, 2.8, and 0.3 sec for *mShab1*, *mShab1*$^{\Delta 565}$, and *fShab*, respectively.

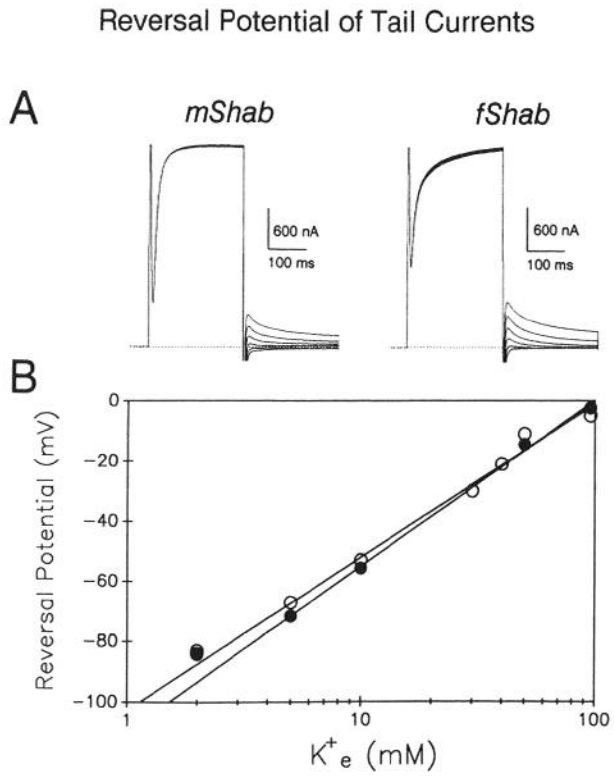

Figure 7. Effect of external potassium ion concentration on current tail reversal potential. *A,* Currents, measured in normal ND96, were elicited by a depolarization to +50 mV followed by repolarizing steps to potentials from −50 to −100 mV. The *dotted line* shows the 0 current level. *B,* Tail current reversal potentials are plotted as a function of external K^+ concentration. The *solid lines* are the best linear regression fits to the data between 5 and 96 mM external K^+. The slopes are 55 and 51 mV per 10-fold change in extracellular K^+ for *mShab1* (*solid circles*) and *fShab,* (*open circles*), respectively; both approximate the theoretical Nernst relationship as expected for a K^+-selective channel. When external K^+ concentration was changed, the concentration of Na^+ was correspondingly changed, in order to keep extracellular monovalent cation concentration constant.

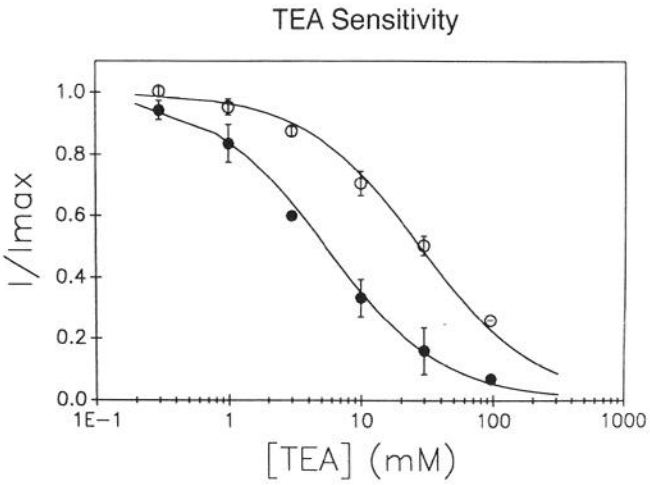

Figure 8. TEA sensitivity of *mShab1* and *fShab* currents. Current amplitude was measured in the presence of variable concentrations of TEA. Data was normalized to a control response in the absence of TEA and plotted versus TEA concentration. Voltage test pulses were to +20 mV from a holding potential of −90 mV. Each *point* is the mean ± SD of 3 independent determinations. *Solid lines* are best fits to inhibition isotherms. Estimated TEA concentrations causing a 50% block were 5 and 27 mM for *mShab1* and *fShab,* respectively.

0.4 sec (n = 3) from 4.2 ± 1.5 sec (n = 6) at −90 mV. At an elevated temperature, 35°C, the rate of recovery (at −90 mV) was approximately 1 sec, indicating a relatively high Q_{10} for this process. A similar temperature dependence was observed for *fShab.*

Similar ion selectivity and pharmacological properties

To assess the ion selectivity of the *mShab1* and *fShab* channels, the reversal potentials of tail currents were measured in different concentrations of external K^+. Figure 7*A* shows an example of current tail reversal in 2 mM external K^+ concentration. Figure 7*B* shows that, as expected for K^+-selective channels, the reversal potential became more depolarized in higher external K^+. Regression analysis for experiments between 5 and 96 mM external K^+ showed slopes of 55 and 53 mV (per 10-fold change in K^+ concentration) for *mShab1* and *fShab,* respectively (Table 1). These values are close to 58 mV, the theoretically expected value for a purely K^+-selective channel.

mShab1 and *fShab* currents were insensitive to 4-AP. Less than 5% of either current was blocked by 3 mM 4-AP. However, *mShab1* and *fShab* were both sensitive to tetraethylammonium chloride (TEA), though *mShab1* channels were about 5–6 times more sensitive to TEA than *fShab* channels (Fig. 8, Table 1).

The conserved functional properties are determined by the conserved structure

Although the *mShab1* and *fShab* amino acid sequences have large nonconserved regions outside of the conserved core, the conserved functional properties appear to be determined by structures within or closely flanking the conserved core of the protein. Hence, we created a truncated version of *mShab1* (*mShab1*$^{\Delta 565}$) that consists mainly of the conserved portions of the channel, and observed the functional properties of the current expressed by the shortened form. The *mShab1* cDNA was cut at the Sph1 site at nucleotide 1691, and a termination codon was added (Figs. 1, 2). This construction removed 293 amino acid residues from the carboxyl end of the protein; most of the remaining 564 amino acids are conserved. Note that the site of truncation in *mShab1* (Fig. 2, arrow) leaves the region having the conserved hydrophobicity profile intact. The amino terminal region of the shortened clone begins at the normal *mShab1* initiator methionine, which is only 10 residues upstream from the conserved region (Fig. 1). The shortened clone ends approximately 80 residues downstream from the end of conservation. Analysis of currents expressed by the shortened form of the channel showed that the measured kinetic, voltage-sensitive, and pharmacological properties did not differ significantly from the values shown in Table 1. An example of the similar behavior of this truncated form is shown in Figures 5 and 6*A,* which shows similar prepulse inactivation properties, inactivation rate, and rate of recovery from inactivation for *mShab1* and *mShab1*$^{\Delta 565}$. However, the average current response of oocytes injected with comparable amounts of cRNA was about 10 times smaller for *mShab1*$^{\Delta 565}$ compared to *mShab1*. The average current amplitude evoked at +20 mV in the same batch of injected eggs was 0.09 ± 0.08 μA (n = 6) for *mShab1*$^{\Delta 565}$ compared to 1.2 ± 0.6 μA (n = 7) for *mShab1*.

Because the major difference between *mShab* and *fShab* is in the rate of recovery from inactivation, we noted with great in-

terest that the recovery from inactivation rate was unaffected by the truncation. In previous studies of the *Shaker* channel (Iverson et al., 1988; Timpe et al., 1988a), the region near the carboxyl terminal had been implicated in determining the rate of recovery from inactivation. Apparently, the sequence removed from *mShab1* does not contain a sequence functionally analogous to that present in the carboxyl terminal region of *Shaker* clones.

Discussion

Shab *delayed rectifier currents are distinct from other cloned channels*

Most of the mammalian *Shaker* subfamily K^+ channels have been categorized as delayed rectifiers because of their slow inactivation, while the fly *Shaker* current is categorized as an A-current because of its rapid inactivation. However, all *Shaker* subfamily channels, whether from fly or mammals, share the common property of very rapid current activation, and all are sensitive to 4-AP (Christie et al., 1989; Stuhmer et al., 1989). These properties contrast with those of *mShab1* and *fShab,* which have slow activation of macroscopic current and are insensitive to 4-AP. Even a mammalian homolog of *Drosophila Shaw* that has been expressed (Yokoyama et al., 1989) activates at a rate that is considerably faster than either *mShab1* or *fShab.* The current–voltage relation of this mammalian *Shaw* homolog also differs from *Shab* currents in that it is considerably shifted to depolarized voltages.

The properties of *mShab1* closely resemble those of a native delayed-rectifier-type potassium channel (I_K) in molluscan neurons (Adams et al., 1980) and in rodent hippocampal neurons (Segal and Barker, 1984). Table 1 is a comparison of several properties between I_K from hippocampal neurons and several cloned K^+ channels. With regard to pharmacological properties, activation "threshold," macroscopic current rise time, current decay, and recovery from inactivation, *mShab1* is the best match. In addition, as seen for *mShab1* (Fig. 6*A*), I_K *in vivo* also undergoes cumulative inactivation (Aldrich et al., 1979). I_K and *mShab,* however, do not seem to match in all measured properties; the major difference is the midpoint of the prepulse inactivation curve (Table 1).

The functional similarities between I_K and *mShab1* are remarkable, but the question may arise as to whether it is valid to compare currents seen *in vivo* with currents expressed in *Xenopus* oocytes. Zagotta et al. (1989) showed that *Shaker* channels behave similarly *in vivo* and in oocytes. Thus, it is possible that I_K is encoded by the *mShab1* gene, but this remains to be seen.

The high degree of interspecies conservation could be an indication that the functional role of this particular potassium channel is highly defined and restricted to a common role in vertebrates and invertebrates. The main function of I_K could be to provide a delayed repolarization of a slow action potential or to provide a delayed termination of a burst of action potentials (Adams et al., 1980; Hille, 1984). In contrast, the *Shaker* homologs, which activate more rapidly, could be involved in more rapid phenomena.

Conservation of mShab1 *and* fShab

mShab1 and *fShab* proteins are, in large part, both structurally and functionally conserved, though neither the conserved structural portions nor the functional properties are identical. The conserved portion contains the proposed transmembrane structures of the channels and, in addition, extends into a region upstream towards the amino terminal that is proposed to be cytoplasmic (Tempel et al., 1987). This region is conserved in all members of the K^+ channel extended gene family (Wei et al., 1990).

The entire extent of conservation between *mShab1* and *fShab* is approximately 470 residues long. Because truncation of the large carboxyl extension of *mShab1* produced no observable alteration of *mShab1* functional properties, the conserved regions and the regions immediately flanking the conserved region are likely to contain virtually all of the structure that is important for determining the measured biophysical properties of the channel. Indeed, this conserved region is only slightly larger than the area of homology common to all proteins coded by the extended gene family of potassium channels (Wei et al., 1990), and, thus, the similar properties of all voltage-gated potassium channels are likely to be determined by structures within this region. The amino acid substitutions between *mShab1* and *fShab* that are present in the conserved core of the proteins appear to be relatively neutral with regard to the voltage-sensitive properties common to *mShab1* and *fShab.*

Relative to the other potassium channel subfamily members, both *mShab1* and *fShab* are large proteins; *mShab1* has an unusually long nonconserved region at the carboxyl end of the protein, while *fShab* is extended on the amino terminal side. The functions of these large regions remain to be determined, but because they do not seem to be involved in determining the kinetic and voltage-sensitive properties that we have measured, other candidate functions may involve subcellular localization or anchoring, pathway of biosynthesis, protein lifetime or turnover rate, or sites of channel modulation. However, the protein sequences we refer to are deduced from the cDNA nucleotide sequence and are based on the assumption that the first AUG of each sequence is the translational start site. The "first AUG rule" holds for hundreds of mRNA sequences that have been analyzed; well over 90% have translational initiation at the first AUG (Kozak, 1987, 1989). *fShab11* has polyglutamine immediately downstream from the putative initiator methionine, which is also found in some *Shaker* proteins (Tempel et al., 1987; Butler et al., 1989). Antibodies directed against a synthetic peptide based on the sequence of this region recognize the *Shaker* channel protein (Schwarz et al., 1990). Additional evidence that the first AUG is the translational start site comes from an analysis of codon bias; our DNA analysis program (MICROGENIE, Beckman), which analyzes codon usage in all 3 reading frames, suggests a high likelihood that both amino and carboxyl termini are translated regions. Although there is considerable circumstantial evidence that translational initiation is at the first AUG of the largest open reading frame in both species, this has not yet been proven.

In comparing kinetic, voltage-sensitive, and pharmacological properties, perhaps the major difference observed between *mShab1* and *fShab* was the rate of recovery from inactivation. In the *Shaker* channel, the rate of recovery from inactivation is modified by residues towards the carboxyl end of the protein (Iverson et al., 1988; Timpe et al., 1988a). The difference observed in the rate of recovery between *mShab1* and *fShab* may also be due to differences at that end of the protein. However, our truncation experiments suggest that, if this is the case, the important structure is likely to be included within the sequence of the shortened version of *mShab1.* This is because the rate of recovery of the shortened version of *mShab1* was not affected by the truncation.

With regard to the differences in current activation delay be-

tween *mShab1* and *fShab*, it is interesting to note that Hodgkin and Huxley (1952b) suggested that the delay in current activation might be directly related to the number of independent gating particles of a channel, and this number might be reflected in the power of the exponential term needed to describe the delay. However, they also recognized that this might be an oversimplification, and that there might be no such simple relationship between kinetics and structure. Even though the 2 channels, *mShab1* and *fShab*, have different activation delays, we assume that these conserved channels have equal numbers of subunits and gate through a mechanistically similar process. Thus, because the exponential terms describing *mShab* and *fShab* current activation require different powers, the numerical values of these powers are not likely to have a simple relationship to channel structure or gating mechanism.

Mouse and rat Shab K^+ *channels: a puzzle*

One unresolved question centers on the differences observed between *mShab1* and a similar *Shab* homolog isolated from rat brain. Even though *mShab1* is similar in sequence to *drk1*, a *Shab* homolog isolated from rat brain (Frech et al., 1989), *mShab1* is much closer to *fShab* in its functional properties than to *drk1*. When expressed in *Xenopus* oocytes, *drk1* codes for a K^+ current that activates at a rate comparable to *mShab1*. However, in contrast to *mShab1* and *fShab*, *drk1* channels activate in a voltage range that is more than 30 mV more depolarized. Also distinct are the pharmacological properties of *drk1*; *mShab1* and *fShab* channels are more than 100 times less sensitive to 4-AP than are *drk1* channels (Table 1). The inactivation properties of *drk1* have not been reported, and, thus, a comparison cannot be made.

Two regions differ between *mShab1* and *drk1*. Seventeen amino acid differences are present on the carboxyl side of the protein, most of which are downstream from the area of conservation between *mShab1* and *fShab*. A second difference is the putative initiator methionine for *mShab1*, which is 4 amino acids upstream from the initiator methionine of *drk1*. Otherwise, the deduced peptides are identical.

Of the 17 amino acid differences on the carboxyl side of *mShab1*, 14 are absent in the truncated form of *mShab1*. Because the truncation of *mShab1* produces no changes in those properties that differ between *mShab1* and *drk1*, it is unlikely that those 14 residues play a role in distinguishing the functional properties of *mShab1* from *drk1*. It is possible that the long carboxyl extension, when present in the *drk1* form, may interact with the conserved structure of the channel, but does not with the substitutions present in *mShab1*. Mutagenesis studies may be necessary to reconcile the functional differences between these 2 channels.

Note added in proof. In light of the recent findings of Mackinnon and Yellen (1990), the fivefold differences in TEA sensitivity between *mShab* and *fShab* could be due to the different residues at mShab 384, Fig. 1.

References

Adams DJ, Smith SJ, Thompson SH (1980) Ionic currents in molluscan soma. Annu Rev Neurosci 3:141–167.

Aldrich RW, Getting PA, Thompson SH (1979) Inactivation of delayed outward current in molluscan neurone somata. J Physiol (Lond) 291:507–530.

Baumann A, Grupe A, Ackermann A, Pongs O (1988) Structure of the voltage-dependent potassium channel is highly conserved from *Drosophila* to vertebrate central nervous systems. EMBO J 7:2457–2463.

Butler A, Wei A, Baker K, Salkoff L (1989) A family of putative potassium channel genes in *Drosophila*. Science 243:943–947.

Butler A, Wei A, Baker K, Salkoff L (1990) *Shal, Shab,* and *Shaw*: three genes encoding potassium channels in *Drosophila*. Nucleic Acids Res 18:2173–2174.

Chandy KG, Williams CB, Spencer RH, Aguilar BA, Ghanshani S, Tempel BL, Gutman GA (1990) A family of three potassium channel genes with intronless coding regions. Science 247:973–975.

Christie MJ, Adelman JP, Douglass J, North RA (1989) Expression of a cloned rat brain potassium channel in *Xenopus* oocytes. Science 244:221–224.

Christie MJ, North RA, Osborne PB, Douglass J, Adelman JP (1990) Heteropolymeric potassium channels expressed in *Xenopus* oocytes from cloned subunits. Neuron 2:405–411.

Connor JA, Stevens CF (1971) Voltage clamp studies of a transient outward membrane current in gastropod neural somata. J Physiol (Lond) 213:21–30.

Frech GC, VanDongen AMJ, Schuster G, Brown AM, Joho RH (1989) A novel potassium channel with delayed rectifier properties isolated from rat brain by expression cloning. Nature 340:642–645.

Grupe A, Schroter KH, Ruppersberg JP, Stocker M, Drewes T, Beckh S, Pongs O (1990) Cloning and expression of a human voltage-gated potassium channel. A novel member of the RCK potassium channel family. EMBO J 9:1749–1756.

Guy RH, Conti F (1990) Pursuing the structure and function of voltage-gated channels. Trends Neurosci 13:201–206.

Hille B (1984) Ionic channels of excitable membranes. Sunderland, MA: Sinauer.

Hodgkin AL, Huxley AF (1952a) Currents carried by both sodium and potassium ions through the membrane of the giant squid axon of Loligo. J Physiol (Lond) 116:449–472.

Hodgkin AL, Huxley AF (1952b) A quantitative description of membrane current and its application to conduction and excitation in nerve. J Physiol (Lond) 117:500–544.

Iverson LE, Tanouye MA, Lester HA, Davidson N, Rudy B (1988) A-type potassium channels expressed from *Shaker* locus cDNA. Proc Natl Acad Sci USA 85:5723–5727.

Kamb A, Tseng-Crank J, Tanouye MA (1988) Multiple products of the *Drosophila Shaker* gene may contribute to potassium channel diversity. Neuron 1:421–430.

Koren G, Liman ER, Logothetis DE, Nadal-Ginard B, Hess P (1990) Gating mechanism of a cloned potassium channel expressed in frog oocytes and mammalian cells. Neuron 2:39–51.

Kornfeld R, Kornfeld S (1985) Assembly of asparagine-linked oligosaccharides. Annu Rev Biochem 54:631–664.

Kozak M (1986) Point mutations define a sequence flanking the AUG initiator codon that modulates translation by eukaryotic ribosomes. Cell 44:283–292.

Kozak M (1987) An analysis of 5'-noncoding sequences from 699 vertebrate messenger RNAs. Nucleic Acids Res 15:8125–8148.

Kozak M (1989) The scanning model for translation: an update. J Cell Biol 108:229–241.

Krebs EB, Beavo JA (1979) Phosphorylation-dephosphorylation of enzymes. Annu Rev Biochem 48:923–959.

Kyte J, Doolittle RF (1982) A simple method for displaying the hydropathic character of a protein. J Mol Biol 157:105–132.

Maniatis T, Fritsch EF, Sambrook J (1982) Molecular cloning: a laboratory manual. Cold Spring Harbor, NY: Cold Spring Harbor Laboratory.

McKinnon D (1989) Isolation of a cDNA clone coding for a putative second potassium channel indicates the existence of a gene family. J Biol Chem 264:8230–8236.

Mackinnon D, Yellen G (1990) Mutations affecting TEA blockade and ion permeation in voltage-activated K^+ channels. Science 250: 276–279.

Pongs O, Kecskemethy N, Muller R, Krah-Jentgens I, Baumann A, Kiltz HH, Canal I, Llamazares S, Ferrus A (1988) *Shaker* encodes a family of putative potassium channel proteins in the nervous system of *Drosophila*. EMBO J 7:1087–1096.

Proudfoot NJ, Brownlee GG (1976) 3' Non-coding region sequences in eukaryotic messenger RNA. Nature 263:211–214.

Saiki RK, Scharf S, Faloona F, Mullis KB, Horn GT, Erlich HA, Arnheim N (1985) Enzymatic amplification of β-globin genomic sequences and restriction site analysis for diagnosis of sickle cell anemia. Science 230:1350–1354.

Salkoff L (1983) Genetic and voltage-clamp analysis of a *Drosophila*

potassium channel. Cold Spring Harbor Symp Quant Biol 48:221–231.

Sanger F, Nicklen S, Coulson AR (1977) DNA sequencing with chain-termination. Proc Natl Acad Sci USA 74:5463–5467.

Schwarz TL, Tempel BL, Papazian DM, Jan YN, Jan LY (1988) Multiple potassium-channel components are produced by alternative splicing at the *Shaker* locus in *Drosophila*. Nature 331:137–142.

Schwarz TL, Papazian DM, Carretto RC, Jan YN, Jan LY (1990) Immunological characterization of K^+ channel components from the *Shaker* locus and differential distribution of splicing variants in *Drosophila*. Neuron 2:119–127.

Segal M, Barker JL (1984) Rat hippocampal neurons in culture: potassium conductances. J Neurophysiol 51:1409–1433.

Solc CK, Zagotta WN, Aldrich RW (1987) Single-channel and genetic analyses reveal two distinct A-type potassium channels in *Drosophila*. Science 236:1094–1098.

Storm JF (1988) Temporal integration by a slowly inactivating K^+ current in hippocampal neurons. Nature 336:379–381.

Stuhmer W, Stocker M, Sakmann B, Seeburg P, Baumann A, Grupe A, Pongs O (1988) Potassium channels expressed from rat brain cDNA have delayed-rectifier properties. FEBS Lett 242:199–206.

Stuhmer W, Ruppersberg JP, Schroter KH, Sakmann B, Stocker M, Giese KP, Perchke A, Baumann A, Pongs O (1989) Molecular basis of functional diversity of voltage-gated potassium channels in mammalian brain. EMBO J 8:3235–3244.

Swanson R, Marshall J, Smith JS, Williams JB, Boyle MB, Follander K, Luneau CJ, Antanavage J, Oliva C, Buhrow SA, Bennett C, Stein RB, Kaczmarek LA (1990) Cloning and expression of cDNA and genomic clones encoding three delayed rectifier potassium channels in rat brain. Neuron 4:929–939.

Tempel BL, Papazian DM, Schwarz TL, Jan YN, Jan LY (1987) Sequence of a probable potassium channel component encoded at *Shaker* locus of *Drosophila*. Science 237:770–775.

Tempel BL, Jan YN, Jan LY (1988) Cloning of a probable potassium channel gene from mouse brain. Nature 332:837–839.

Timpe LC, Jan YN, Jan LY (1988a) Four cDNA clones from *Shaker* locus of *Drosophila* induce kinetically distinct A-type potassium currents in *Xenopus* oocytes. Neuron 1:659–667.

Timpe LC, Schwarz TL, Tempel BL, Papazian DM, Jan YN, Jan LY (1988b) Expression of functional potassium channels from *Shaker* cDNA in *Xenopus* oocytes. Nature 331:143–145.

Wei A, Covarrubias M, Butler A, Baker K, Pak M, Salkoff L (1990) Potassium current diversity is produced by an extended gene family conserved in *Drosophila* and mouse. Science 233:780–782.

Yokoyama S, Imoto K, Kawamura T, Higashida H, Iwabe N, Miyata T, Numa S (1989) Potassium channels from NG108-15 neuroblastoma-glioma hybrid cells. FEBS Lett 259:37–42.

Zagotta WN, Hoshi T, Aldrich RW (1989) Gating of single *Shaker* channels in *Drosophila* muscle and in *Xenopus* oocytes injected with *Shaker* mRNA. Proc Natl Acad Sci USA 86:7243–7247.